minerals

MDPI

Article

Factors Affecting the Upgrading of a Nickeliferous Limonitic Laterite Ore by Reduction Roasting, Thermal Growth and Magnetic Separation

Filipe Rodrigues, Christopher A. Pickles *, John Peacey, Richard Elliott and John Forster

The Robert M. Buchan Department of Mining, Queens's University, Kingston, ON K7L3N6, Canada; 7fmr@queensu.ca (F.R.); john.peacey@queensu.ca (J.P.); richard.elliott@utoronto.ca (R.E.); john.forster@mail.utoronto.ca (J.F.)

* Correspondence: christopher.pickles@queensu.ca; Tel.: +1-613-533-2759

Received: 25 July 2017; Accepted: 19 September 2017; Published: 20 September 2017

Abstract: There is considerable interest in the development of new processes to extract the nickel from the oxidic nickeliferous laterite deposits, as the global nickel sulphide resources are rapidly becoming more difficult to access. In comparison to sulphide ores, where the nickel-containing mineral can be readily concentrated by flotation, nickel laterites are not amenable to significant upgrading, due to their complex mineralogy. In this paper, firstly, a brief overview of the conventional techniques used to process the nickeliferous limonitic laterites is given, as well as a review of current research in the area. Secondly, a thermodynamic model is developed to simulate the roasting process and to aid in the selection of process parameters to maximize the nickel recovery and grade and also to minimize the magnetite content of the concentrate. Thirdly, a two-stage process involving reduction roasting and thermal growth in either a tube furnace or a rotary kiln furnace, followed by magnetic separation, was investigated. Thermogravimetric, differential thermal and mineral liberation analyses techniques were utilized to further understand the process. Finally, the nickel grades and recovery results were compared to those available in the literature.

Keywords: laterites; limonite; nickel; reduction roasting; magnetic separation

1. Introduction

Nickel metal is primarily employed in high nickel alloys and superalloys. Nickel utilization is increasing at a rate of about 4% per year [1]. Nickel is used in stainless steels, non-ferrous alloys and plating applications. In the earth's crust, nickel can exist in either sulphidic or oxidic form. As a consequence of the declining worldwide nickel sulphide supply, there is increasing interest in the economic development of the nickeliferous laterite deposits, which represent about 59.5% of the known nickel resources [2]. The nickel laterite ores are mainly found in Australia, the Philippines, and Indonesia. These deposits are located close to the surface of the earth and therefore are mined using surface mining methods. Since the nickel oxide is in solid solution in the host rock, it is not feasible to produce a high grade concentrate using flotation [3]. Additionally, it has been reported that the environmental damage associated with extracting the nickel from these oxide deposits is greater than that for sulphide deposits [4].

There are two main types of nickel laterite deposit: limonite and saprolite. These are separated by a layer of smectite clay. The nickel concentrations in these layers are roughly 1% to 1.6% for limonite, 2% to 5% for saprolite and 1% to 1.5% for smectite [5]. The upper limonitic layer of the deposit consists of mainly goethite ((Fe,Ni)O·OH) with some hematite (Fe_2O_3) and some magnesium silicates. These ores contain substantial amounts of water, and the nickel has traditionally been extracted via hydrometallurgical processes. Another approach for the processing of these ores for the

successful recovery of the nickel and potentially the cobalt would be to selectively reduce all the nickel and cobalt oxides and some of the iron oxide via low temperature solid state reduction to produce an intermediate product, known as ferronickel. This reduced product could be further upgraded downstream, by removing the unreduced oxides, so as to produce a concentrate, and magnetic separation could be considered as a suitable method for concentration. One problem in such a process, particularly with the limonitic ores, is the formation of magnetite, which will contaminate the ferronickel concentrate, thereby diluting the nickel grade. In the present paper, the existing industrial practices are discussed along with previous research performed on the reduction roasting and magnetic separation of the nickeliferous limonitic laterites. A thermodynamic model is utilized to predict the grade and recoveries of the ferronickel and also the grade of the concentrate. Experimental results obtained in both a stationary tube furnace and a rotary kiln are discussed and compared to the other results available in the literature. Thermogravimetric, differential thermal and mineral liberation analyses techniques were utilized to further understand the reduction process.

2. Current Industrial Practices

Presently, there are three commercial processing routes for nickel laterite ores as shown in Figure 1 and the method selected depends on the ore composition. Limonitic ores are typically processed by hydrometallurgical leaching methods in order to avoid the high costs associated with dehydrating, heating and smelting of a large volume of relatively low grade ore. In some cases, limonitic ores may be smelted in a blast furnace to produce nickel pig iron, although this is an energy intensive process, with a high volume waste stream, and generally yields low quality products [6]. The most common method for treating limonitic ores is High Pressure Acid Leaching (HPAL), although other leaching methods have been employed [7]. Nickel bearing ore is leached with sulphuric acid in an autoclave, followed by the recovery of nickel metal from the solution by electrowinning or hydrogen reduction. A high purity nickel metal can be produced by this method, and nickel recoveries are typically in the range of 90% to 92% [8]. While several of these processes have been implemented, operating costs have been high and production levels unsatisfactory [8,9]. In addition to the high acid consumption, the resultant waste stream is a significant environmental concern [4]. The Caron process uses a combined pyro/hydrometallurgical approach to produce a high-grade ferronickel from limonite/saprolite blended feeds. Because of the low recoveries and high operating costs, the Caron process is generally considered to be uneconomic [1,10]. Each of these three processing options faces different challenges, although in general they are costly, energy intensive and produce a high volume waste stream. A low cost method of producing a nickel concentrate could significantly reduce the operating costs of the current nickeliferous laterite processing methods.

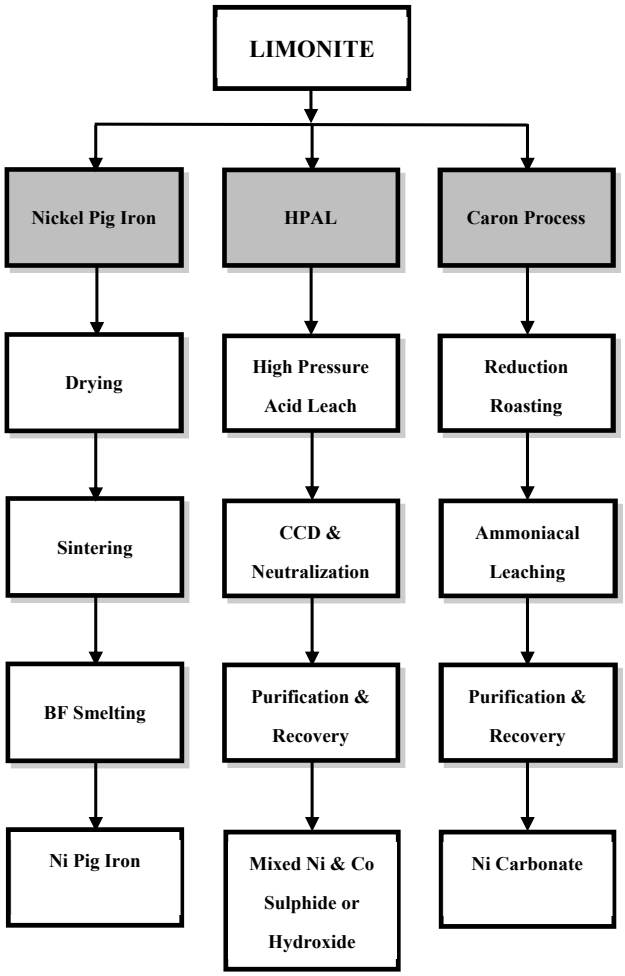

Figure 1. Simplified flowsheet of the current commercial production methods for the extraction of nickel from nickeliferous limonitic laterite ores, adapted from previous work by Dalvi et al. [1].

3. Previous Experimental Research

3.1. Reduction Roast and Upgrade

Various degrees of success in selectively reducing and upgrading limonitic ores at the experimental bench scale level have been achieved. De Graaf [11] showed that selective reduction of limonite to the magnetite/wustite phase boundary was possible using a CO/CO_2 and H_2/H_2O reducing atmosphere. The presence of water vapour in the reducing atmosphere was found to have a deleterious effect on the extraction of nickel. Using hydrogen and carbon monoxide as reductants in both a tube furnace and a fluidized bed, Antola et al. [12] were able to produce a high grade (70% to 80% Ni) product by solid state selective reduction. Pure metallic nickel could not be produced by selective reduction, as the nickel was always found in a nickel-iron alloy phase. Low partial pressures of reducing gas with relatively short processing times provided the optimum nickel grade. Varying the temperature in the range of 700 to 1000 °C had little effect on the reduction selectivity although reduction proceeded faster at higher temperatures. Reduction occurred five to seven times faster in the fluidized bed compared to the tube furnace. The authors proposed that the ferronickel could be magnetically separated.

Zevgolis et al. [13] reviewed the physicochemical properties of the reduction roasting of Greek laterite ores. The researchers concluded that the reduction degrees of the iron and nickel oxides in Greek laterites between 700 to 900 °C could not exceed 33% and 76%, respectively, even though adequate amounts of carbon remained in the calcine. The reduction was finished after 20 to 40 min due

to the formation of iron silicates such as fayalite ($2FeO{\cdot}SiO_2$) and forsterite (Mg_2SiO_4), which coated the oxide grains, impeding further reduction. Valix and Cheung [14] studied the phase transformations of laterite ores under reducing conditions and temperatures up to 800 °C. When limonite ores were reduced, the mineral phases formed were magnetite, taenite and fayalite. Taenite is an iron-nickel alloy mineral containing 20% to 65% nickel. X-Ray Diffraction (XRD) patterns showed that taenite becomes more dominant as the temperature increased from 650 to 750 °C, but upon further heating, the taenite disappeared. On cooling the reduced limonite from 800 to 25 °C in air, there were no evident changes in the phases, suggesting the stability of the phases formed at higher temperatures. They also conducted leaching tests using an ammoniacal leach and achieved an optimum nickel recovery of 80% at 600 °C.

Kawahara et al. [15] investigated the reducibility of laterite ores using hydrogen over a temperature range of 400 to 1000 °C. The reducibility was based on the degree of reduction of the oxides of iron, nickel and cobalt to their metallic forms. The nickel reduction degree varied from 19% to 70%, and the reduction process was concluded after 40 min. The reducibility of nickel oxide increased with increasing temperature and the iron content of the ore. The magnesia and silica in the ore combined together to form olivine ($(Mg,Fe,Ni)_2SiO_4$), and Ni^{2+} was substituted for Mg^{2+} in the silicate matrix. The activity of nickel oxide in the silicate solid solution is low, and this explained the poor reducibility using gaseous reductants.

The effect of precalcination on the reducibility of the limonitic ore in a H_2/CO_2 atmosphere was studied by O'Connor et al. [16]. The function of precalcination was to dehydroxylate goethite. During calcination, the goethite became more porous and the surface area of the ore increased, exposing the reduced nickel phase for recovery via an ammoniacal leach solution. Under reducing conditions, the goethite was dehydroxylated to hematite, and then reduced to magnetite at 500 °C. The formation of taenite and fayalite simultaneously occurred at this temperature. Precalcination produced recrystallized hematite, which was less susceptible to reduction and this resulted in reduced ferronickel formation. Utigard and Bergman [17] found that with pretreatment of the ore in air or nitrogen followed by reduction in an H_2/CO_2 atmosphere, the limonite ore was easier to reduce to the metallic state.

Valix and Cheung [14] found that a prolonged reduction period resulted in over-reduction of limonite, resulting in decreased nickel recovery. Reoxidation of the reduced wustite phase to magnetite impeded the effectiveness of magnetic separation to remove the gangue. Chander and Sharma [18] found that cooling in an inert atmosphere prevented reoxidation to magnetite. The reoxidation was limited to the surface layers of the sample. Quenching the samples in either water or air resulted in extensive reoxidation.

3.2. Effect of Sulphur

A number of studies have been performed on the effects of sulphur-containing additives on the reduction and/or recovery of nickel from nickeliferous laterite ores. Sulphur has been added in various forms such as: elemental sulphur, pyrite or pyrrhotite or sodium sulphate. In general, it has been shown that sulphur additions are beneficial in terms of both improved nickel grade and nickel recovery. A number of researchers have concluded that the addition of elemental sulphur promotes the growth of ferronickel particles during the selective reduction of the saprolite ores [19–22].

With regards to the addition of elemental sulphur, it would be expected that as the limonitic ore is heated, the elemental sulphur is converted to sulphur gas and a large proportion would escape. However, a fraction would react with hematite to form pyrite (FeS_2) as follows:

$$Fe_2O_3 + 2.75S_{2(g)} = 2FeS_2 + 1.5SO_{2(g)} \quad (1)$$

or under reducing conditions:

$$Fe_2O_3 + 2.5S_{2(g)} + CO_{(g)} = 2FeS_2 + SO_{2(g)} + CO_{2(g)} \quad (2)$$

At higher temperatures, the pyrite decomposes to pyrrhotite (FeS) as follows:

$$FeS_2 = FeS + S_{2(g)} \quad (3)$$

In a patent by Diaz et al. [23], where the sulphur additions to a limonitic ore were in the range of 2% to 4%, it was postulated that the ferronickel particles form via a Fe-S-O liquid phase. This liquid phase could facilitate the agglomeration of the ferronickel particles. In many cases, the ferronickel particles are found associated with an FeS-rich phase, possibly indicating the ferronickel particles precipitated on cooling [19,20,22–24]. Also, it has been shown that when sulphur is added, the ferronickel particles are larger [20,22]. Since some iron is sulphidized, the iron content of the ferronickel alloy is reduced and consequently, the nickel grade is increased [25].

From a kinetic perspective, the release of the gaseous sulphur could open up the mineral structure and facilitate dehydroxylation [26]. Also, this would increase the particle surface area available for gaseous reduction. The fissures/voids that remain after sulphur volatilization could provide nucleation sites for ferronickel particle growth. It has also been suggested that sulphur can reduce the surface tension of the ferronickel particles, enhancing the agglomeration process [27]. Valix and Cheung [21] reported an increase in the nickel recovery from 29% to 81% for a precalcined limonitic ore initially containing 5 wt % sulphur. Thus, although sulphur additions to limonitic ores have been shown to lead to larger ferronickel particles, improved recoveries and higher grades, there is little consensus on the mechanism or mechanisms by which these improvements are achieved.

3.3. Thermodynamic Considerations

Of interest in the reduction roasting and the concentration of the limonitic laterites are the nickel grades and recoveries in the ferronickel. Furthermore, if the ferronickel is concentrated by magnetic separation, then the behavior of magnetite needs to be considered. From a thermodynamic perspective, it would be expected that the major factors affecting the grade, the recovery and the amount of magnetite, would be as follows: the ore composition and any additives, the reduction temperature, the type of reducing agent and the amount of reducing agent per unit of ore. Previously, a thermodynamic model has been developed for the limonitic ores [28], and it is utilized here to determine the influence of variables on the grades and recoveries and in particular, the amount of magnetite, for the particular ore composition utilized in this research. A ferronickel phase containing some cobalt was assumed to form, while the other condensed species were considered to be part of the oxide phase. Activity coefficient data available in the literature for various species were utilized as described previously [28–30]. The ore was mainly composed of goethite, but for the purposes of the calculation, the ore was assumed to be dewatered, and therefore the iron content was reported as 91.88% hematite (Fe_2O_3). The nickel oxide (NiO) content was 1.62% and the minor impurities were silica (SiO_2), magnesia (MgO) and alumina (Al_2O_3).

Figure 2 shows the calculated nickel recovery as a function of the amount of carbon added and also the reaction temperature. The carbon addition is represented as kg of carbon per 100 kg of ore. At low carbon additions (less than 1.5 kg/100 kg) and across the whole temperature range, metallic nickel was not formed, as the carbon was utilized to reduce the hematite to magnetite. As the carbon addition approached 2 kg/100 kg, metallic nickel began to be recovered. For all carbon additions, metallic nickel did not form until about 400 °C. However, for the lower carbon additions, reoxidation could occur at higher temperatures, which lowered the nickel recovery. Above about 600 °C and for carbon additions of over about 4 kg/100 kg, nickel recoveries approaching 100% were readily achieved. Figure 3 shows the nickel grade in the ferronickel alloy as a function of the amount of carbon added and also the reaction temperature for the same conditions as in Figure 2. The nickel grade was inversely proportional to the amount of metallic iron in the ferronickel. Since NiO was less stable than FeO, then metallic nickel should be selectively reduced, to some degree, at reduction potentials which were less reducing than those for the formation of metallic iron. Again, at temperatures below about

400 °C and carbon additions below about 1.5 kg/100 kg, there was no metallic nickel. However, as the conditions became more reducing in terms of both the temperature and carbon additions, then the nickel grades rose quite dramatically, to values approaching 95%. Consequently, over both a range of carbon additions and a range of temperatures, nickel grades could approach 95%. However, these conditions were short-lived as metallic iron was produced in increasing amounts with both increasing temperature and carbon additions. By inspection of Figures 2 and 3, it can be seen that both high grades and high recoveries can be achieved at above 600 °C. For these reasons, 600 °C was used as the primary roasting temperature in this work. Above 600 °C, the nickel recoveries approached 100%, but the nickel grade dropped with increasing temperature to a relatively constant value of 3% to 5%.

The behaviour of magnetite is shown in Figure 4, again as a function of temperature and carbon additions. From room temperature upwards, the amount of magnetite increased as the hematite was reduced and reached a maximum at about 200 °C for all carbon additions. Subsequently, the amount of magnetite decreased as wustite began to form with increasing temperature and the amount was essentially independent of the amount of carbon added until about 600 °C, where the amount of carbon had a strong influence. At higher temperatures, the amount of magnetite decreased with increasing carbon addition and for any given temperature, the amount of magnetite was linearly dependent on the carbon addition. A carbon addition of about 7 kg/100 kg corresponded to the stoichiometric requirement for the reduction of all the NiO to Ni metal and all of the Fe_2O_3 to FeO as given by the following reactions:

$$NiO + C = Ni + CO_{(g)} \quad (4)$$

$$Fe_2O_3 + C = 2FeO + CO_{(g)} \quad (5)$$

At high temperatures and high carbon additions, the magnetite is reduced to wustite and metallic iron, while at lower temperatures, only wustite forms in decreasing amounts with decreasing temperature. These results indicate that the amount of magnetite is a complex function of both the carbon addition and the temperature. A comparison of Figures 2–4 shows that if intermediate temperatures are utilized to achieve both high nickel recoveries and grades, then the amount of magnetite is also high. Additionally, even if the amount of magnetite formed at high temperatures is small, on cooling, the wustite and metallic iron revert to magnetite under equilibrium conditions. Consequently, the amount of magnetite in the reduced product would be high and essentially independent of the reduction conditions. Therefore, to minimize the amount of magnetite at room temperature it would be necessary to quench the reduced material and/or cool in a controlled atmosphere. Also, reoxidation could occur at room temperature and therefore in the present research, sample analysis was performed as quickly as possible.

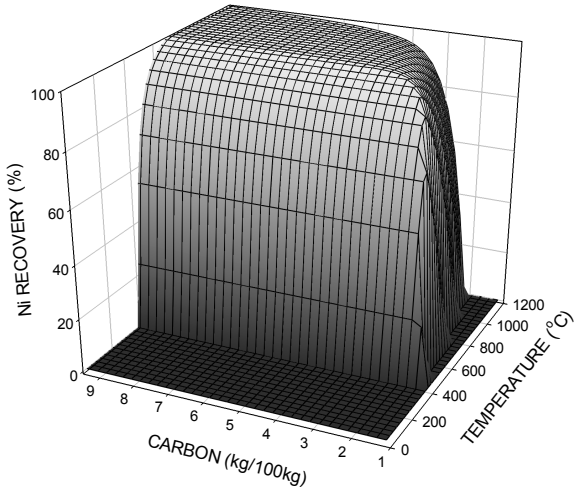

Figure 2. Effects of temperature and carbon additions on the nickel recovery for the limonitic ore.

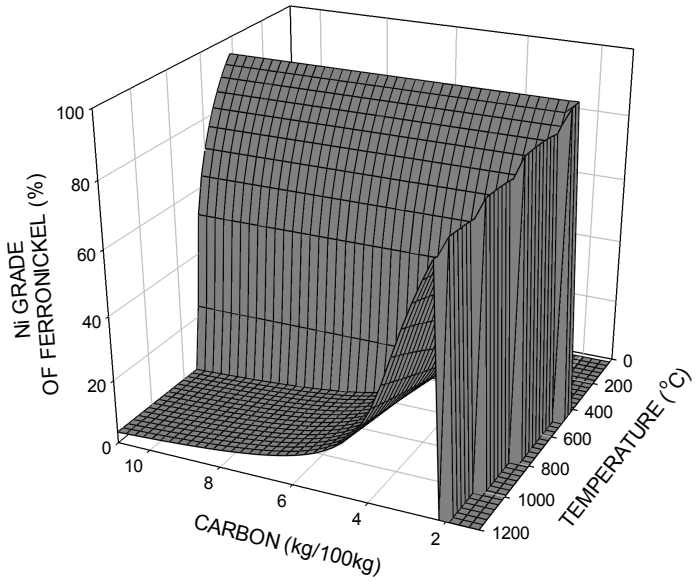

Figure 3. Effects of temperature and carbon additions on the nickel grade of the limonitic ore.

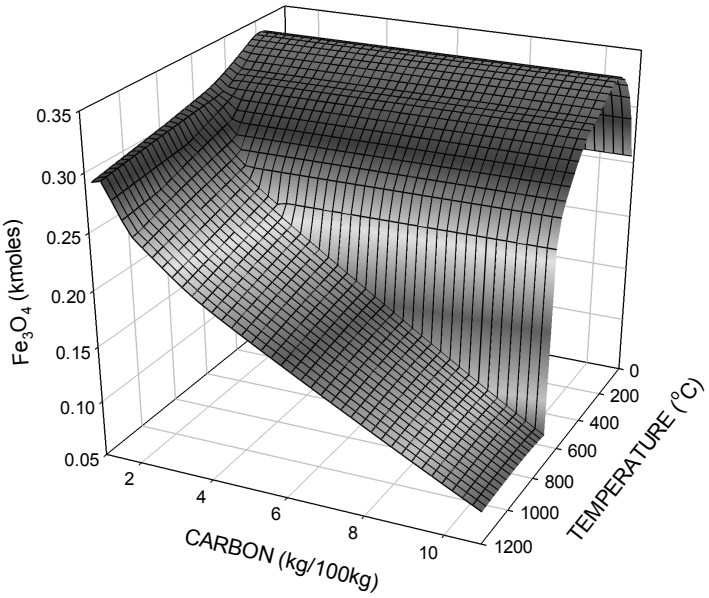

Figure 4. Effects of temperature and carbon additions on the amount of magnetite for the limonitic ore.

Figure 5 shows the nickel grade of the simulated concentrate as a function of the amount of carbon added and the reduction temperature. Here, the concentrate was assumed to consist of the ferronickel alloy plus magnetite. Again at low temperatures and low carbon additions, there was no nickel produced. Above about 400 °C, the nickel grade increased rapidly. At relatively low temperatures and/or carbon additions, the amounts of wustite and metallic iron were low, while the amount of magnetite was high, which lowered the grade. On the other hand, at high carbon additions and/or temperatures, the amount of metallic iron was high, which again lowered the grade. Consequently, the nickel grade of the simulated concentrate was relatively uniform over most of the reduction conditions and varied in the range of about 1.5% to 2%.

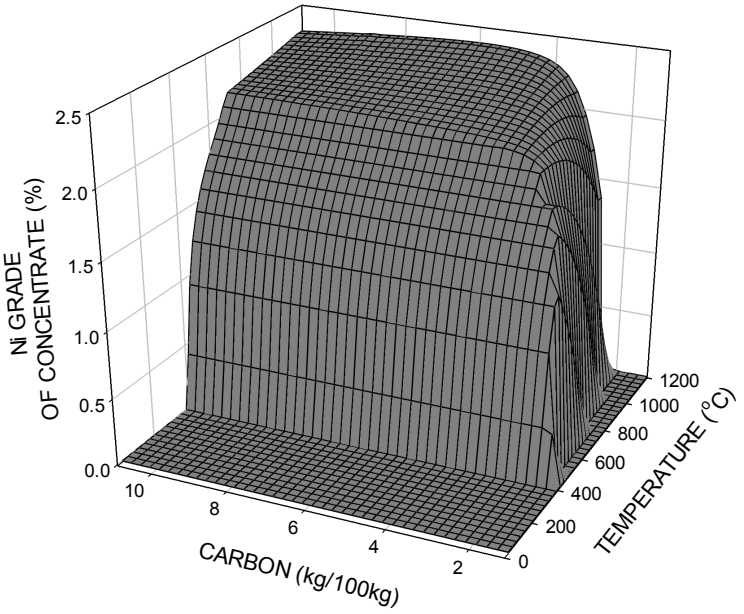

Figure 5. Effects of temperature and carbon additions on the grade of the magnetic concentrate (Fe + Ni + Co + Fe_3O_4) for the limonitic ore.

4. Experimental methods

4.1. Raw Materials

The as-received ore was dried at 100 °C for seven days to ensure the removal of free water. Two kilograms of the ore were crushed and separated into eight representative samples of approximately 180 g using a riffle splitter. Subsequently, the ore was pulverized in a ring pulverizer for 15 s and then screened to a size passing 100 mesh (150 µm). Oversized material was repulverized for an additional 5 s then rescreened until one hundred percent of the sample was minus 100 mesh. In order to maintain the ore in a dry condition prior to use in the reduction experiments, the screened samples were stored at 65 °C in a drying oven.

The chemical analysis of the dried limonitic ore is provided in Table 1. The dried ore had a nickel oxide content of 1.48%, a very high iron content (58.71%) and low concentrations of magnesia (MgO), silica (SiO_2) and alumina (Al_2O_3), which are typical of the nickeliferous limonitic ores. X-Ray Diffraction (XRD) analysis identified goethite (FeO·OH) as the major mineral phase present in the limonitic ore. On a dehydroxylated basis, the calculated iron oxide (Fe_2O_3) and nickel oxide (NiO) contents were 91.88% and 1.62%, respectively.

Table 1. Analysis of the dried limonitic ore.

Species	NiO	CoO	Total Fe	SiO_2	MgO	Al_2O_3
(wt %)	1.48	0.045	58.71	2.15	0.22	2.92

For the experiments, the limonitic ore was mechanically mixed with predetermined amounts of bituminous coal and sulphur. The composition of the bituminous coal is given in Table 2. Reagent grade elemental sulphur was used. In order to promote both gas-solid and solid-solid reactions, the reagents and the ore were compacted together. The ore, coal and sulphur mixture, with a total mass of 3 g, was briquetted at a pressure of 55.2 MPa into 1.3 cm diameter cylinders with a height of 1.0 cm. Initially, a single briquette was utilized. However in later tests, three briquettes were combined to give a total sample mass of 9 g and five briquettes were combined to give a sample mass of about 15 g. The control briquette contained 6% bituminous coal and 4% sulphur.

Table 2. Chemical analysis of the bituminous coal.

Component	Total Carbon	Fixed Carbon	Volatiles	Moisture	Ash	Sulphur
(%)	73.0	51.6	36.6	1.2	7.9	2.3

4.2. Stationary Tube Furnace Experiments

A schematic diagram of the tube furnace utilized for the thermal upgrading of the ore is shown in Figure 6. The process comprised of two isothermal stages: roasting at 600 °C followed by thermal particle growth at either 1000 or 1100 °C. A quartz tube in a horizontal resistance furnace was used as the reaction chamber. The sample was placed in a quartz boat, which was lined with magnesium oxide powder to minimize the reaction of the sample with the boat. The furnace was then sealed at both ends and purged with high purity nitrogen gas at a flow rate of 300 mL/min throughout the experiment. After initial purging, the hot zone temperature was increased by 20 °C/min to 600 °C and the boat containing the sample was introduced into the hot zone and reacted for 60 min. Subsequently, the hot zone temperature was ramped at 20 °C/min to reach the particle growth temperature of 1000 or 1100 °C. The samples were held at the growth zone temperature for 60 min then withdrawn to the cool zone for 40 min. The temperature of the cooled sample ranged from 60 to 80 °C. Magnetic separation and subsequent analysis were performed immediately after removing the processed samples from the furnace in order to minimize reoxidation.

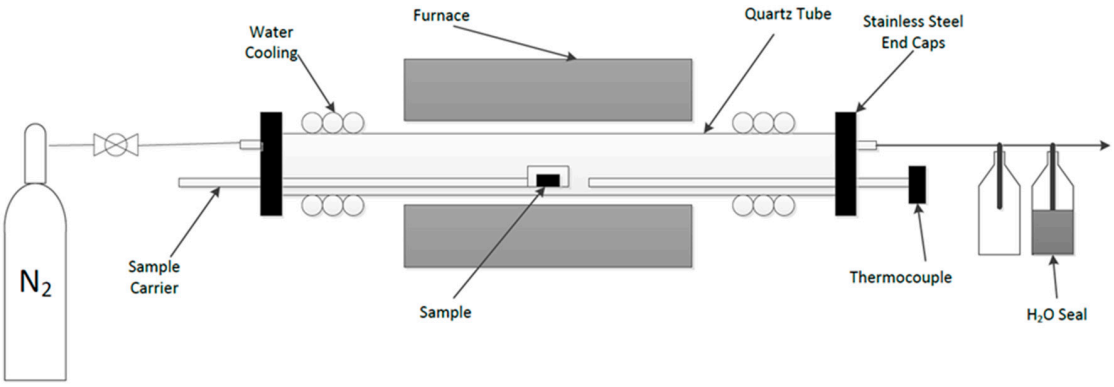

Figure 6. Schematic diagram of the tube furnace.

4.3. Rotary Kiln Experiments

In order to obtain larger and more representative samples for the subsequent magnetic separation tests, experiments were performed in a rotary kiln, which is shown in Figure 7.

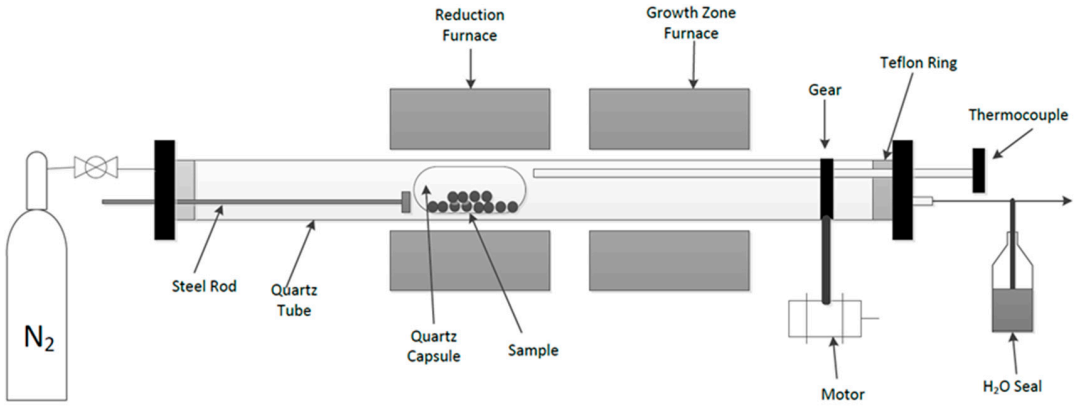

Figure 7. Schematic diagram of the rotary kiln.

The kiln rotated at a constant speed of 2 rpm. Two separate resistance furnaces were placed around the kiln to establish both the reduction zone at 600 °C and the growth zone at 1000 °C. Nitrogen was introduced into the kiln at a rate of 1.5 L/min in order to maintain a neutral atmosphere. A charge consisting of one hundred of the 3 g briquettes (300 g in total) was placed inside a quartz capsule and inserted into the kiln. The capsule had openings at both ends to allow both the purge gas to pass through and the reaction gases to escape. Initially, the capsule was held in the cooling zone at the front of the furnace while the temperature of the reaction zone was ramped up to the set point temperature. The capsule was then moved into the reaction zone for 60 min and then into the growth zone for another 60 min. After completion of the two-stage process, the capsule was withdrawn into the cool zone until it could be safely handled.

4.4. Magnetic Separation Tests

Magnetic separation tests were performed to test the viability of upgrading the processed samples to a ferronickel concentrate. Prior to magnetic separation, the processed samples were pulverized using a ring pulverizer to enhance liberation of the reduced material. The samples were pulverized for 20 s and then passed through a 200 mesh (74 μm) screen. Oversized material was repulverized for an additional 5 s then rescreened. Water was added to the minus 200 mesh material prior to magnetic separation to produce a slurry. Initial magnetic separation test work was performed using a Davis Tube Tester (DTT). In the DDT tests, the sample mass was 10 g and the magnetic field strength was fixed at 4800 G at various water flowrates and rotation speeds. In order to able to vary the magnetic field intensity, additional magnetic separation studies were conducted using Wet High Intensity Magnetic Separation (WHIMS). Outokumpu Technology's (Espoo, Finland) Carpco WHIMS Model 3x4L (Serial number 227-05) was utilized and here the magnetic field intensity could be varied from 0 to 17.5 kG. The magnetic media used was 6.4 mm iron spheres, and this matrix media provide a large surface area, which is more suited for collecting small magnetic particles and also minimizes entrapment of non-magnetic material.

4.5. Analytical Techniques

The chemical compositions of the samples were determined using wet analytical techniques. Total digestion of the samples was performed using aqua regia and the solutions were analyzed for nickel and iron using a Thermo Fisher Scientific (Waltham, MA, USA) iCE 3000 Series Atomic Absorption Spectroscopy (AAS) unit. Powder X-Ray Diffraction (XRD) was used to characterize the mineralogy of the raw materials and selected processed samples. An Xpert Pro Phillips powder diffractometer (Almelo, The Netherlands) with Cu kα radiation linked with the commercial software X-pert High Score was utilized. Scanning Electron Microscopy (SEM) was performed using a Mineral Liberation Analysis (MLA) 650 FED Environmental SEM (Hillsboro, OR, USA). Back scattered electron imaging was the primary mode used to analyze the samples. Energy dispersive X-Ray spectroscopy (EDS) helped verify the chemical composition of the mineral phases detected. Thermogravimetric and Differential Thermal Analysis (TGA/DTA) studies were conducted using a Netzsch STA 449 F3 Jupiter system (Selb, Germany). The samples were processed in 5 mL alumina crucibles. In order to simulate the actual reduction experiments, samples were ramped at 20 °C/min or 50 °C/min then held at a reduction temperature of 600 °C for 60 min and then ramped at 20 °C/min to a thermal growth temperature of 1000 or 1100 °C for 60 min. A neutral atmosphere was maintained by using nitrogen as the carrier gas at flowrates of 50 to 150 mL/min.

5. Results and Discussion

5.1. Thermogravimetric and Differential Thermal Analysis

Figure 8 shows the TGA results for the samples containing 6% coal and 4% sulphur for a reduction temperature of 600 °C and thermal growth temperatures of either 1000 or 1100 °C. If all of the iron

in the ore were present as goethite, then the mass loss due to dehydroxylation would be about 9.5%. Up to 600 °C, the mass loss was much higher at about 15%, and this additional 5.5% mass loss could mainly be attributed to the evaporation of the majority of the sulphur and some reduction. During the isothermal hold at 600 °C, there was only a small mass loss, typically less than 1%. Considerable mass loss and thus reduction occurred during the second heating stage up to the thermal growth temperatures, particularly for the sample heated to 1100 °C. This was attributed to the presence of residual reductant. For the sample at 1000 °C, additional reduction occurred during the initial stages of the isothermal hold. For the sample at 1100 °C there was little mass loss during the hold; however, there was an overall additional 5% mass loss, and this was indicative of considerable over-reduction and excessive formation of metallic iron. As a major research objective was to avoid the formation of significant metallic iron, most of the roasting tests were performed with the lower thermal growth temperature of 1000 °C.

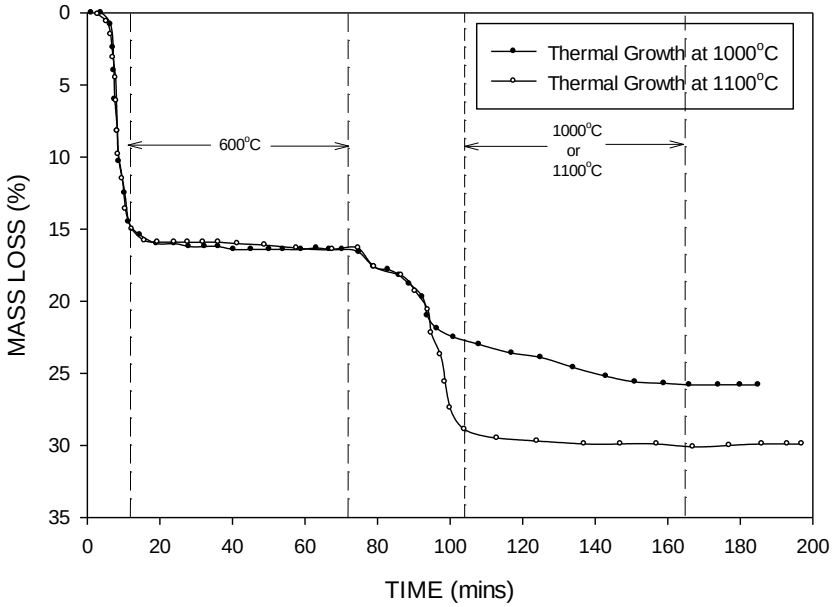

Figure 8. TGA results of mass loss versus time for reduction at 600 °C and thermal growth at 1000 or 1100 °C for a sample containing 6% coal and 4% sulphur.

Figure 9 shows both the TGA and DTA curves, where the sample was again heated to 600 °C for 60 min and then heated to a thermal growth temperature of 1000 °C, but in this case, excess sulphur and coal were added so as to amplify their effects. A mixture of limonite, coal and sulphur was used with a mass ratio of 2:1:1. Again, the majority of the mass loss occurred during the two heating stages. During the first heating stage, the mass loss was about 27%, and this was due to dewatering, the removal of some sulphur and some reduction. Again, at the roasting temperature of 600 °C, the mass loss was only about 1%, with the majority of this occurring within the first ten minutes. During heating from 600 to 1000 °C, a further mass loss of about 2% was observed. Another mass loss of about 1% occurred at the thermal growth temperature of 1000 °C and subsequently the sample mass remained constant. The DTA curve showed two endothermic peaks: (1) one at about 296 °C, corresponding to the very large mass loss due to the dehydroxylation of goethite, (2) and a second at 490 °C corresponding to the decomposition of pyrite to pyrrhotite. During cooling of the sample, an exothermic peak was observed at 908 °C. In the Fe-FeS system, the melting temperature of the eutectic composition is 988 °C at 1 atm, and thus this peak could be due to the solidification of the proposed Fe-O-S melt. This would support the proposal by Diaz et al. [23] that a Fe-S-O liquid forms, which facilitates the growth of the ferronickel particles. It should be noted that DTA evidence of melting or partial melting of the sample was not observed during the heating stage.

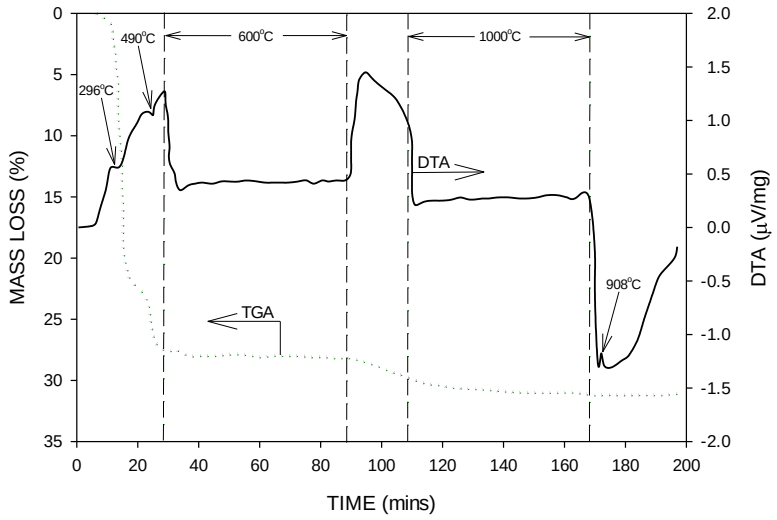

Figure 9. TGA/DTA results for reduction at 600 °C and thermal growth at 1000 °C for a mixture of limonite, coal and sulphur with a mass ratio of 2:1:1.

5.2. Magnetic Separation Using Davis Tube Tester (DTT)

Several preliminary tests were performed using the DTT to magnetically separate the concentrate. The effect of sulphur additions, particle growth zone temperature and the difference between the as-received ore and calcined ore (at 600 °C) were investigated. However, there was no significant difference between the results. There were very little tailings with 90% of the feed reporting as magnetics to the concentrate. The average analyses of the concentrate from these tests were as follows: 1.35% Ni and 77.2% Fe. The nickel and iron recoveries were 87.0% and 89.9%, respectively. The high percentage magnetics, the low nickel grades and the high iron recoveries indicated that separation was not efficient. Similar problems were encountered by Iwasaki et al. [31], who used X-Ray Diffraction analysis of the roasted material to confirm that the presence of a small amount of magnetite in the wustite was sufficient to prevent efficient magnetic separation. Thus, in the current research, all subsequent magnetic separation tests were performed using WHIMS.

5.3. Magnetic Separation Using Wet High Intensity Magnetic Separation (WHIMS)

Figure 10 shows the percent magnetics as a function the magnetic field strength for the WHIMS tests. The percent magnetics increased from about 20% at 2 kG to about 60% at 14 kG. These values were considerably lower than the 90% magnetics obtained with the DTT, and this indicates improved separation. Figure 11a,b show the effect of magnetic field strength on the nickel grade and recovery and the iron grade and recovery, respectively. At low magnetic field strengths of about 2 kG, the nickel grade was about 4%, and this indicated considerable concentration of the nickel. As the magnetic field strength increased, the nickel grade decreased rapidly and at much higher magnetic field strengths of about 14 kG, the grade was similar to that of the as-received ore. At 2 kG, the nickel recovery was about 65% and decreased somewhat to about 55% at 14 kG. For the case of iron, the grade decreased only slightly with increasing magnetic field strength and had an average value of 79.9%. On the other hand, the iron recovery increased rapidly from about 10% at 2 kG to about 70% at 14 kG. These results indicated that that the highest nickel grades and recoveries were achieved at low field strengths. As the field strength increased, more iron was recovered, and therefore, the nickel grade decreased. Consequently, in subsequent tests a field strength of 3 kG was utilized.

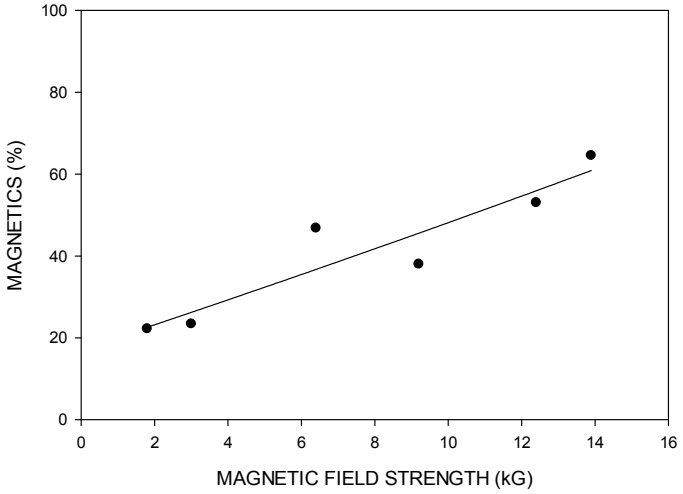

Figure 10. Percent magnetics as a function of magnetic field strength for WHIMS.

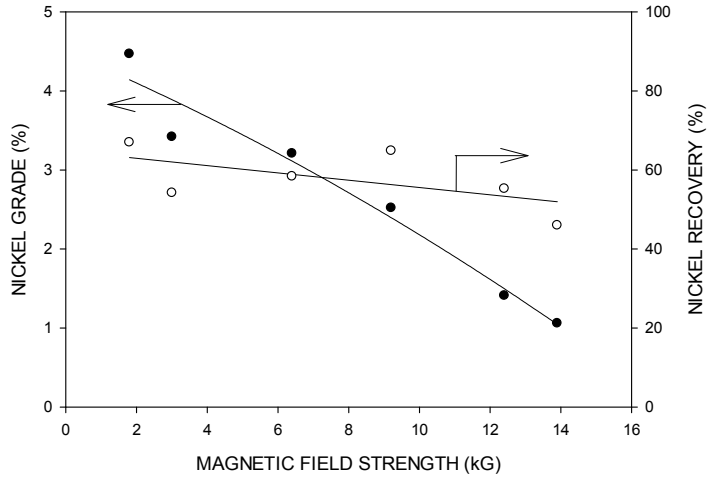

(**a**)

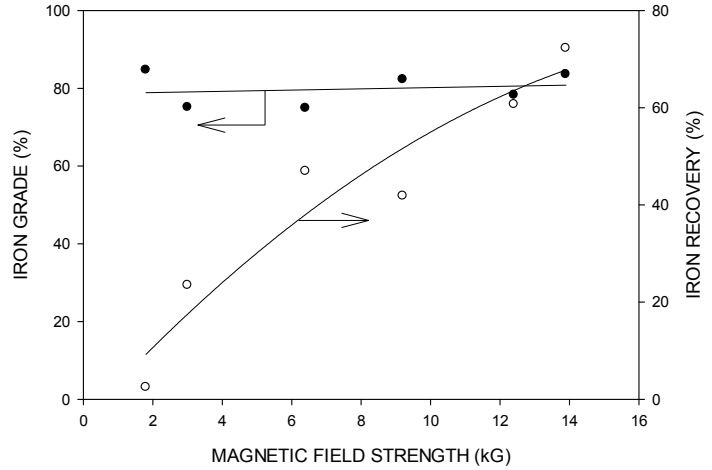

(**b**)

Figure 11. (**a**) Effect of magnetic field strength on nickel grade and recovery; (**b**) Effect of magnetic field strength on iron grade and recovery.

Figure 12 shows the effect of sulphur additions on the percent magnetic material. Initially, the amount of magnetics increased only modestly with sulphur but then more intensively as the sulphur addition increased. Figure 13a,b show the effect of sulphur on the nickel grade and recovery and the iron grade and recovery, respectively. Sulphur additions promoted both increased nickel grades and recoveries. In a manner similar to the percent magnetics, both the nickel grade and the nickel recoveries first increased modestly with sulphur addition and then more intensively. The iron recovery also initially increased modestly with sulphur additions and then more intensively. Consequently, the increased iron recovery limited the increase in the grade of the concentrate, despite the increasing nickel recovery. The iron grade showed only a slight increase with sulphur addition. These results show that increasing sulphur additions result in increased nickel and iron recoveries but the increase is higher for nickel than iron, and thus the nickel grade increases. The increase in iron grade with increasing sulphur would suggest improved separation of the gangue constituents.

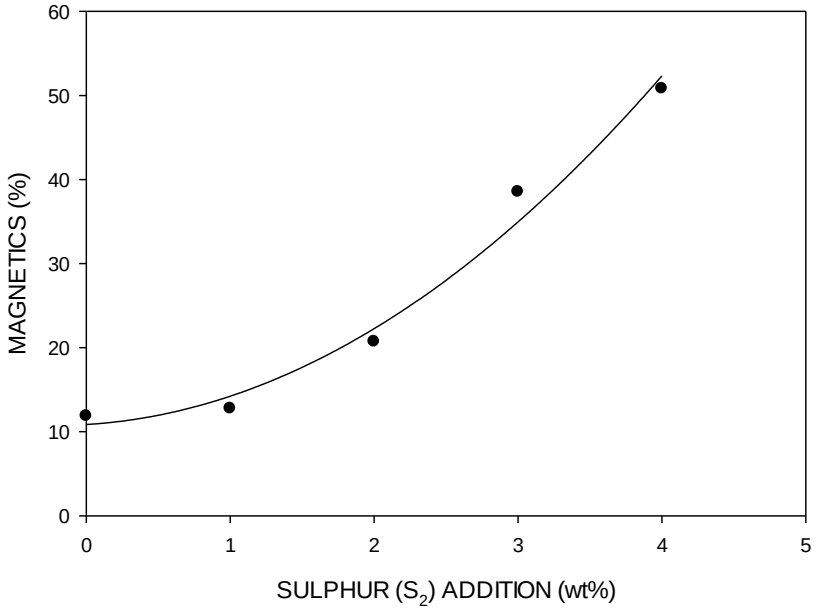

Figure 12. Effect of sulphur additions on the percent magnetic material.

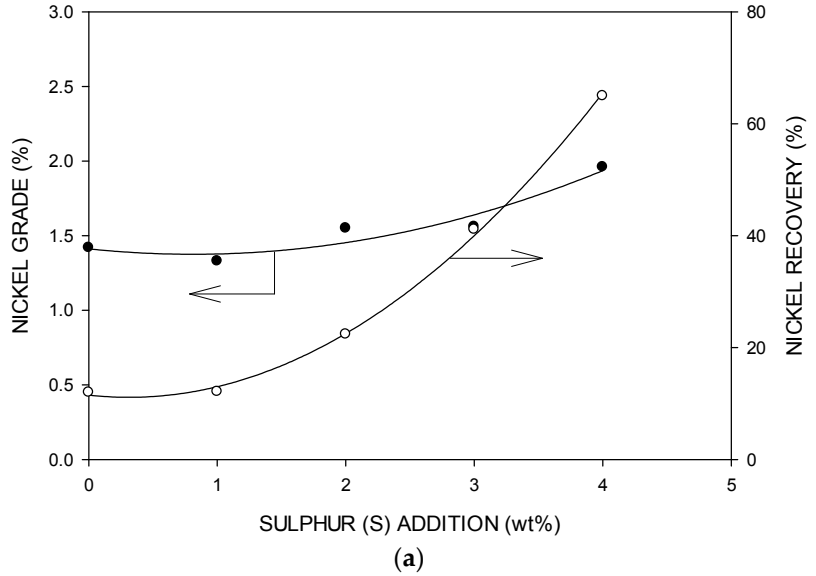

(**a**)

Figure 13. *Cont.*

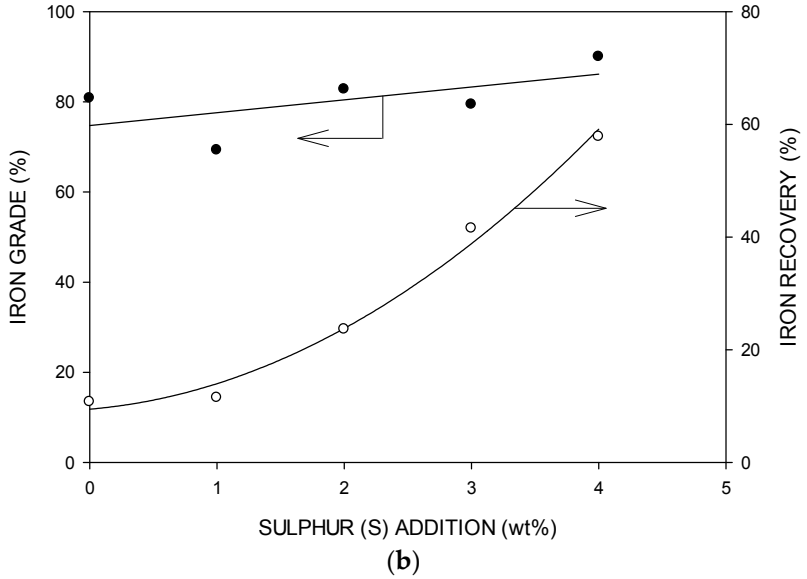

Figure 13. (**a**) Effect of sulphur additions on nickel grade and recovery at a magnetic field strength of 3 kG; (**b**) Effect of sulphur additions on the iron grade and recovery at a magnetic field strength of 3 kG.

Figure 14a,b show the MLA results for the cumulative percent passing as a function of particle size for various nickel grade ranges, for the briquettes containing 6% coal and 6% coal plus 4% sulphur, respectively and Figure 15 shows the cumulative 80% passing size (d_{80}) versus the nickel grade ranges for the two cases. For both the sulphurless and the sulphur-containing samples, it can be seen that ferronickel particles are produced with widely varying nickel grades and as the particle size decreases then the nickel grade increases. This would indicate that as the particles grow then the nickel grade decreases, suggesting that a major factor affecting particle growth is both the formation of additional metallic iron and incorporation into the growing ferronickel particles. For the sulphurless sample, the largest particles are observed for the grade range of 0% to 2% Ni, with a maximum size of 53 μm and a d_{80} of about 9 μm. For the higher nickel grade ranges, the curves are significantly shifted to much lower particle sizes, with both the curves and the d_{80} values shifting slightly to lower sizes as the grade increases. The range of d_{80} values for these grades was very narrow and varied from about 3.5 to 2.5 μm. Thus, magnetic separation of this material would preferentially remove the larger particles, which would have a nickel grade of less than 2%. For the sample containing sulphur, although the maximum size for the 0% to 2% Ni range curve has shifted from 53 μm to a lower particle size of 38 μm, the d_{80} value has increased from 9 to 18 μm. Also, the d_{80} values for the other nickel grade curves have shifted from the range of 3.5 to 2.5 μm for the sulphurless samples to larger values of 17 to 8.5 μm. Thus, in contrast to the sulphurless sample, the curve for the 0% to 2% nickel grade range is more closely associated with the other curves. These larger particle sizes for the sulphur-containing sample would be expected to lead to improved recovery and higher grades during magnetic separation.

Figure 16 shows an X-ray diffraction pattern of a sample reduced at 600 °C and held for thermal growth at 1100 °C. The species detected were wustite (FeO), kamacite (FeNi with Ni $\leq$ 10%), fayalite (Fe_2SiO_4), magnesioferrite ($Mg(Fe^{3+})_2O_4$) and pyrrhotite (FeS). The main constituent was wustite, demonstrating that the conditions were sufficiently reducing so as to minimize the formation of magnetite. The detection of kamacite was indicative of the presence of the ferronickel alloy. Fayalite formed as a result of the reaction of some of the iron oxide with silica and also, some of the iron oxide reacts with magnesium oxide to form magnesioferrite, which is magnetic. Pyrrhotite was detected which demonstrates that the majority of the sulphur is present as FeS.

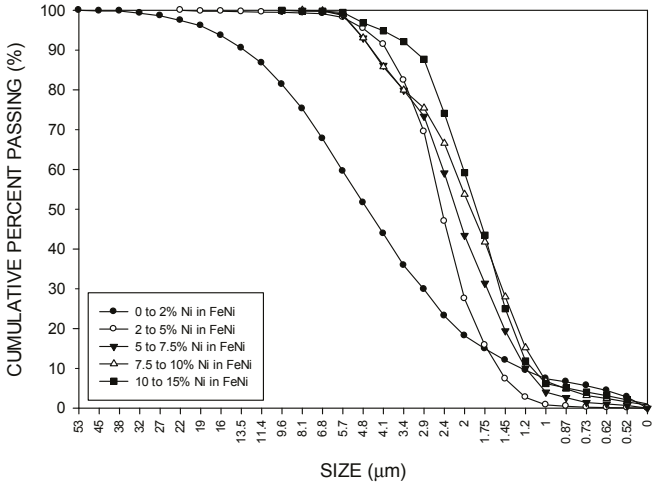

(**a**)

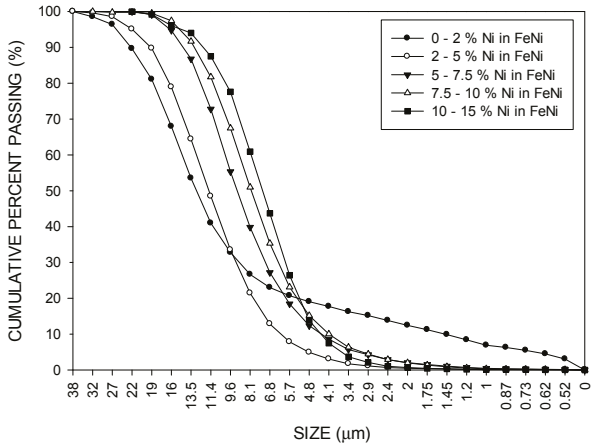

(**b**)

Figure 14. (**a**) Results of the MLA studies showing the cumulative percent passing as a function of particle size for various nickel grade ranges for the briquette containing 6% coal; (**b**) Results of the MLA studies showing the cumulative percent passing as a function of particle size for various nickel grade ranges for the briquette containing 6% coal plus 4% sulphur.

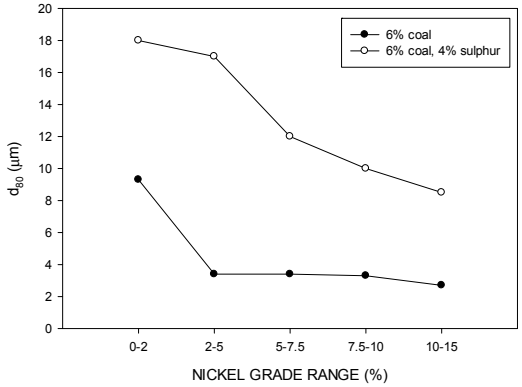

Figure 15. Effect of nickel grade range on the cumulative 80% passing size (d_{80}) as a function of the nickel grade range for the sample containing 6% coal and the sample containing 6% coal plus 4% sulphur.

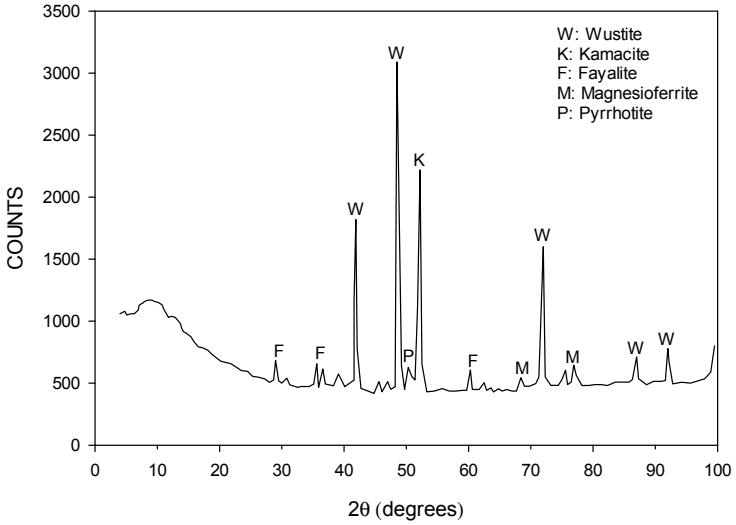

Figure 16. X-Ray Diffraction pattern of a reduced briquette at 600 °C with a thermal growth temperature of 1100 °C.

5.4. Nickel Grade and Recovery

Typically, in both the tube furnace and the rotary kiln tests, the nickel recoveries were only about 65%, and therefore, additional magnetic separation tests were performed on the tailings to determine if improved nickel recovery could be achieved. The metal grades and recoveries for the rotary kiln tests are shown in Figure 17a,b. A rougher and two scavenger stages were performed. In the rougher stage, the nickel and iron grades were 4.31% and 85.1%, respectively. In the first scavenger stage, the nickel recovery to the concentrate increased by 14.8% and in the second by 5.4% to give an overall nickel recovery of 86.5%. The nickel grade of the final concentrate was 3.2% and contained 80.9% iron. The overall iron recovery to the final concentrate was 27.9%, and the iron grade was 80.9%. Somewhat similar results were obtained for the tube furnace tests as shown in Figure 18a,b. The nickel grades of the rougher concentrate and the final concentrate were 4.16% and 3.87%, respectively. Meanwhile, the iron grades of the rougher concentrate and the final concentrate were both 90.3%. The nickel recoveries of the rougher concentrate and the final concentrate were 64.2% and 83.6%, respectively. The corresponding iron recoveries were 26.0% and 39.8%. Thus, in order to obtain nickel recoveries of about 85% to the final concentrate and nickel grades in the range of 3.2% to 3.8%, three concentration stages were required. Under these conditions, 30% to 40% of the iron was recovered with iron grades in the final concentrate of 80% to 90%.

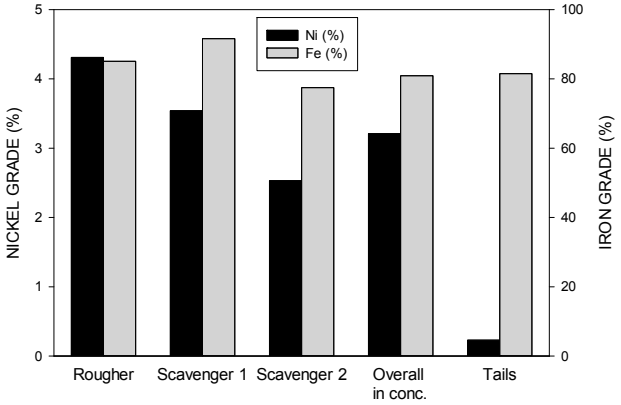

(**a**)

Figure 17. *Cont.*

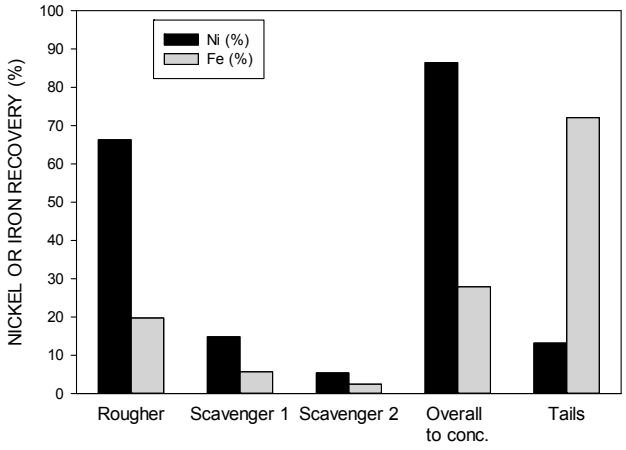

(**b**)

Figure 17. (**a**) Nickel and iron grades in the concentrates and tails for the rotary kiln tests; (**b**) Nickel and iron recoveries in the concentrates and tails for the rotary kiln tests.

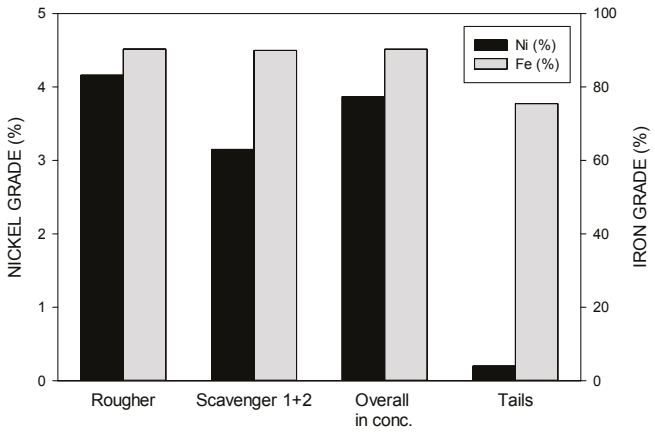

(**a**)

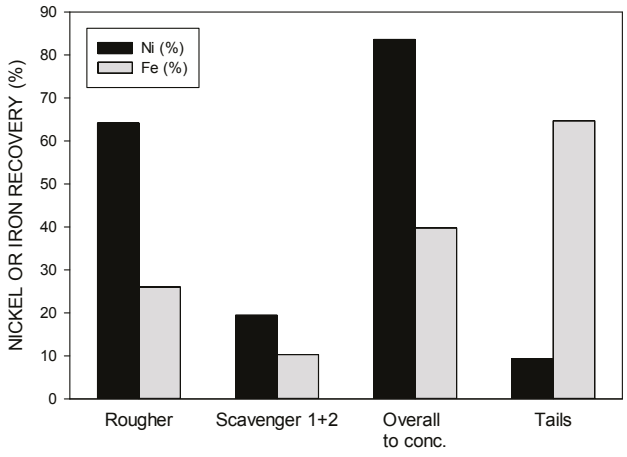

(**b**)

Figure 18. (**a**) Nickel and iron grades in the concentrates and tails for the tube furnace tests; (**b**) Nickel and iron recoveries in the concentrate and tails for the tube furnace tests.

6. Conclusions

(1) A thermodynamic model was developed to describe the carbothermic reduction roasting process of a limonitic laterite ore using HSC Chemistry 7.1 and was utilized to predict the grade of the ferronickel alloy and the nickel recovery to the ferronickel alloy. The grade and recovery were studied as a function of the carbon addition and reduction temperature. Since it was proposed to utilize a reduction roast followed by magnetic separation to concentrate the nickel, then the effects of operating parameters on the formation of magnetite were investigated. Nickel recoveries approaching 100% and nickel grades from 3% to 5% could be achieved at temperatures above 600 °C. A significant amount of magnetite formed at high temperatures and on cooling, reversion occurred. Thus, either quenching or rapid cooling under a controlled atmosphere was recommended.

(2) TGA/DTA studies were performed on the ore plus carbon plus sulphur mixture for a temperature profile, which consisted of heating to two isothermal steps, one for reduction at 600 °C for 60 min and another for particle growth at 1000 or 1100 °C for 60 min, followed by cooling. The TGA curves showed that the majority of the mass loss occurred during heating to 600 °C, and this was attributed to dehydroxylation, evaporation of sulphur and some reduction. Also, some mass loss and therefore reduction occurred during heating to 1000 °C. There was only a small amount of mass loss during the two isothermal stages. The DTA curve showed three peaks: (1) an endothermic peak at about 296 °C, corresponding to a very large mass loss due to the dehydroxylation of goethite, (2) an endothermic peak at 490 °C corresponding to the decomposition of pyrite to pyrrhotite, and (3) an exothermic peak at 908 °C, which could be due to the solidification of the proposed Fe-O-S melt.

(3) Magnetic separation using the Davis Tube Tester was not successful with most of the nickel, and also most of the iron reporting to the magnetics and thus the nickel grade was low. Improved results were obtained using Wet High Intensity Magnetic Separation. The nickel grades and recoveries decreased with increasing field strengths, but at low kG in the range of 2 to 4, nickel grades in the range of 3% to 4% and nickel recoveries in the range of 60% to 70% could be achieved.

(4) The effects of sulphur additions on the grade and recovery of both nickel and iron were investigated. The addition of sulphur significantly improved the nickel recovery, and also there was a slight improvement in grade. Similarly, the iron recovery increased but was not as pronounced as that for nickel and the iron grade increased only slightly. This demonstrated improved separation of the gangue constituents. Mineral Liberation Analysis of the reaction product demonstrated that with the addition of sulphur, the ferronickel particles were larger and had a higher grade, which would explain the improvements in recovery and grade in the magnetic separation process.

(5) Although high nickel grades could be achieved in the concentrate with one pass through the WHIMS, the nickel recovery was low and in the range of 60% to 70%. Therefore, second and third scavenger stages were performed on the tailings. For the tube furnace tests, the final nickel grade was 3.87% and the nickel recovery was 83.6%. Similar results were obtained in the rotary kiln tests with a nickel grade of 3.2% and recoveries of 86.5%.

(6) It is recommended that future research be directed towards optimizing the additives usage as well as the separation processes.

Acknowledgments: The authors wish to thank the Natural Sciences and Engineering Research Council of Canada (NSERC) and XSTRATA for their support of this research. In addition, Kingston Process Metallurgy (KPM) is acknowledged for the use of their rotary kiln. The authors thank William Anthony for his assistance in preparing the manuscript.

Author Contributions: Filipe Rodrigues, Richard Elliott and John Forster performed the experimental work. John Peacey was the principal supervisor of the project. Christopher A. Pickles performed the analysis of the results and the interpretation of the data.

Conflicts of Interest: The authors declare no conflict of interest.

References

1. Dalvi, A.D.; Bacon, W.G.; Osborne, R.C. The past and the future of nickel laterites. Presented at the PDAC 2004 International Conference Trade Show and Investors Exchange, Toronto, ON, Canada, 7–10 March 2004; pp. 1–27.
2. Mudd, G.M.; Jowitt, S.M. A detailed assessment of global nickel resource trends and endowments. *Econ. Geol.* **2014**, *109*, 1813–1841. [CrossRef]
3. Farrokhpay, S.; Filippov, L. Challenges in processing nickel laterite ores by flotation. *Int. J. Miner. Process.* **2016**, *151*, 59–67. [CrossRef]
4. Mudd, G.M. Nickel sulfide versus laterite: The hard sustainability challenge remains. Proceedings of 48th Annual Conference of Metallurgists, Sudbury, ON, Canada, 23–26 August 2009; pp. 1–10.
5. Butt, C.R.M.; Cluzel, D. Nickel laterite ore deposits: Weathered serpentinites. *Elem. Int. Mag. Miner. Geochem. Petrol.* **2013**, *9*, 123–128. [CrossRef]
6. Zhang, Y.; Zhou, Y.; Zhaoyi, L.Z. Technical analysis of producing low Ni pig iron with laterite in a blast furnace. *Baosteel Tech. Res.* **2008**, *2*, 36–40.
7. Norgate, T.; Jahanshahi, S. Assessing the energy and greenhouse gas footprints of nickel laterite processing. *Miner. Eng.* **2011**, *24*, 698–707. [CrossRef]
8. Kyle, J. Nickel laterite processing technologies—Where to next? Presented at the ALTA 2010 Nickel/Cobalt/Copper Conference, Perth, WA, Australia, 24–27 May 2010.
9. Whittington, B.I.; Muir, D. Pressure acid leaching of nickel laterites: A review. *Miner. Process. Extr. Metall. Rev.* **2000**, *21*, 527–599. [CrossRef]
10. Rhamdhani, M.A.; Hayes, P.C.; Jak, E. Nickel laterite part 2: Thermodynamic analysis of phase transformations occurring during reduction roasting. *Miner. Process. Extr. Metall. Trans. Inst. Min. Metall. C* **2009**, *118*, 146–155. [CrossRef]
11. De Graaf, J.E. The treatment of lateritic nickel ores—A further study of the Caron process and other possible improvements. Part I. Effect of reduction conditions. *Hydrometallurgy* **1979**, *5*, 47–65. [CrossRef]
12. Antola, O.; Holappa, L.; Paschen, P. Nickel ore reduction by hydrogen and carbon monoxide containing gases. *Miner. Process. Extr. Metall. Rev.* **1995**, *15*, 169–179. [CrossRef]
13. Zevgolis, E.; Zografidis, C.; Halikia, I. The reducibility of the Greek nickeliferous laterites: A review. *Miner. Process. Extr. Metall. Trans. Inst. Min. Metall. C* **2010**, *119*, 9–17. [CrossRef]
14. Valix, M.; Cheung, W.H. Study of phase transformation of laterite ores at high temperature. *Miner. Eng.* **2002**, *15*, 607–612. [CrossRef]
15. Kawahara, M.; Toguri, J.M.; Bergman, R.A. Reducibility of laterite ores. *Metall. Trans. B* **1988**, *19*, 181–186. [CrossRef]
16. O'Connor, F.; Cheung, W.H.; Valix, M. Reduction roasting of limonite ores: Effect of dehydroxylation. *Int. J. Miner. Process.* **2006**, *80*, 88–99. [CrossRef]
17. Utigard, T.; Bergman, R.A. Gaseous reduction of laterite ores. *Metall. Trans. B* **1992**, *23*, 271–275. [CrossRef]
18. Chander, S.; Sharma, V.N. Reduction roasting/Ammonia leaching of nickeliferous laterites. *Hydrometallurgy* **1981**, *7*, 315–327. [CrossRef]
19. Jiang, M.; Sun, T.; Liu, Z.; Kou, J.; Liu, N.; Zhang, S. Mechanism of sodium sulfate in promoting selective reduction of nickel laterite ore during reduction roasting process. *Int. J. Miner. Process.* **2013**, *123*, 32–38. [CrossRef]
20. Li, G.; Shi, T.; Rao, M.; Jiang, T.; Zhang, Y. Beneficiation of nickeliferous laterite by reduction roasting in the presence of sodium sulfate. *Miner. Eng.* **2012**, *32*, 19–26. [CrossRef]
21. Valix, M.; Cheung, W.H. Effect of sulfur on the mineral phases of laterite ores at high temperature reduction. *Miner. Eng.* **2002**, *15*, 523–530. [CrossRef]
22. Zhu, D.Q.; Cui, Y.; Vining, K.; Hapugoda, S.; Douglas, J.; Pan, J.; Zheng, G.L. Upgrading low nickel content laterite ores using selective reduction followed by magnetic separation. *Int. J. Miner. Process.* **2012**, *106*, 1–7. [CrossRef]
23. Diaz, C.M.; Vahed, A.; Shi, D.; Doyle, C.D.; Warner, A.E.M.; MacVicar, D.J. Low Temperature Thermal Upgrading of Lateritic Ores. U.S. Patent US5178666 A, 12 January 1993.
24. Liu, J.; Liu, S.; Ju, S.; Du, W.; Pan, F.; Yang, S. The effect of sodium sulphate on the hydrogen reduction process of nickel laterite ore. *Miner. Eng.* **2013**, *49*, 154–164. [CrossRef]

25. Kukura, M.E.; Stevens, L.G.; Auck, Y.T. Development of UOP process for oxide silicate ores of nickel and cobalt. Presented at the International Laterite Symposium, New Orleans, Lousiana, USA, 1979; pp. 527–552.
26. Dean, J.G. Nickel Ore Reduction Process Using Asphalt Additive. U.S. Patent US2913331 A, 17 November 1959.
27. Canterford, J.H. The treatment of nickeliferous laterites. *Miner. Sci. Eng.* **1975**, *7*, 3–15.
28. Elliott, R.; Pickles, C.A.; Forster, J. Thermodynamics of the reduction roasting of nickeliferous laterite ores. *J. Miner. Mater. Charact. Eng.* **2016**, *4*, 320–346. [CrossRef]
29. Pelton, A.D.; Schmalzried, H.; Sticher, J. Computer-assisted analysis and calculation of phase diagrams of the Fe-Cr-O, Fe-Ni-O and Cr-Ni-O systems. *J. Phys. Chem. Solids* **1979**, *40*, 1103–1122. [CrossRef]
30. Swartzendruber, L.J.; Itkin, V.P.; Alcock, C.B. The Fe-Ni (iron-nickel) system. *J. Phase Equilibria* **1991**, *12*, 288–312. [CrossRef]
31. Iwasaki, I.; Takahasi, Y.; Kahata, H. Extraction of nickel from iron laterites and oxidized nickel ores by a segregation process. *Metall. Trans.* **1966**, *235*, 308–320.